RESEARCH ARTICLE

Check for updates

Oxidation of phenols by the excited state of an osmium(VI) nitrido complex†

Yu-Zhong Lu, [ID] [a] Li-Xin Wang,[a] Rui-Yue Qi,[a,b] Jing Xiang, [ID] *[a] Ji-Yan Liu*[a] and Tai-Chu Lau [ID] *[a,c]

The photoreaction of an osmium(VI) nitrido complex, $[Os^{VI}(N)(L)(CN)_3]^-$ (**OsN**), with various phenols has been investigated. Upon irradiation of **OsN** with visible light, the excited state (**OsN***) is generated which reacts readily with a variety of phenols. **OsN*** reacts with mono- and di-substituted phenols, including 2,6-dimethylphenol, 2,6-dichlorophenol and 4-methylphenol to afford the corresponding osmium(II) benzoquinone monoimine and osmium(IV) benzoquinone monoiminato complexes. On the other hand, in the reactions of **OsN*** with bulky tri-substituted phenol such as 2,4,6-tri-*tert*-butylphenol, C−C bond cleavage occurred and $[Os^{IV}(L)(CN)_3(N={}^tBu_2Ph_{(-2H)}O)]^-$ was formed as the major product. The electronic effects of various *para*-substituents (X) on the oxidation of phenols were investigated by the method of initial rates (R_x). A Hammett plot of $\log(R_x/R_H)$ *versus* σ_p is linear with a ρ value of −0.54. A linear correlation of $\log(R_x)$ with the oxidation potentials (E) of phenols was also found with a slope of −0.80. On the other hand, no correlations were found between $\log(R_x)$ and O−H bond dissociation energy (BDE), as well as the pK_a of phenols. The oxidation of phenols by **OsN*** exhibits a negligible kinetic isotope effect (KIE), $k(C_6H_5OH)/k(C_6D_5OD) \sim 1$. These results are consistent with a mechanism that involves an initial 1e⁻ oxidation of the phenol followed by rapid proton transfer (ET-PT) to generate a phenoxy radical, this is followed by a N-rebound step to give the osmium products.

Introduction

Transition metal nitrido (M≡N) complexes are intermediates in N₂ fixation and potentially useful reagents for the nitrogenation of organic substrates.[1,2] Compared to metal oxo (M=O) species, there are relatively few nitrido complexes that are reactive towards common organic substrates. Examples include osmium(VI) nitrido complexes containing various N-based ligands such as 2,2′-bipyridine (bpy), 2,2′:6′,2″-terpyridine (tpy), and tris(1-pyrazolyl)methane (tpm); they are highly electrophilic and readily undergo N-atom transfer to a variety of organic substrates.[3] Moreover, Ru(VI) nitrido complexes bearing salen type ligands, such as $[Ru^{VI}(N)(salchda)(CH_3OH)]^+$ (**RuN**, salchda = N,N′-bis(salicylidene)-o-cyclohexyl-diamine dianion),[4] and several iron(V/IV)[5] and Mn(V/VI)[6] nitrido complexes are also highly reactive species that are capable of oxidizing various organic substrates.

The oxidation of phenols to quinones by various oxidants has been extensively studied, mainly because such reactions are relevant to many biological processes.[7–13] Phenols can be oxidized by various pathways (Fig. 1), the most common one is initial 1e⁻ oxidation resulting in the formation phenoxy radicals, which is followed by rapid loss of the phenolic proton (consecutive electron transfer-proton transfer, ET-PT). Further rapid loss of 1e⁻ + 1H⁺ results in the formation of quinones.[14,15] On the other hand, oxidation of phenols by some metal oxo species may involve an H-atom transfer mechanism (or concerted ET-PT).[16–22] Oxidation *via* an initial electrophilic attack on the aromatic ring of phenol has also been reported for a ruthenium(IV) species.[23,24]

Prior to this work, there was only one example on oxidation of phenols by a metal nitrido species. **RuN** readily reacts with phenols in the presence of pyridine to afford (salchda)ruthenium(II) *p*-benzoquinone imine complexes.[25] The reactions were proposed to proceed *via* an initial electrophilic attack by **RuN** at the aromatic ring of phenols.

In an attempt to design a highly active metal nitrido complex, we turned our attention to the excited state chemistry of M≡N. We reported recently the synthesis of a highly luminescent Os(VI) nitrido complex, $[Os^{VI}(N)(L)(CN)_3]^-$

[a]Key Laboratory of Optoelectronic Chemical Materials and Devices (Ministry of Education), School of Optoelectronic Materials and Technology, Jianghan University, Wuhan, 430056, China. E-mail: xiangjing35991@sohu.com
[b]Hebei Key Laboratory of Heterocyclic Compounds, Handan University, Handan 056005, Hebei Province, China
[c]Department of Chemistry, City University of Hong Kong, Tat Chee Avenue, Kowloon Tong, Hong Kong, P. R. China. E-mail: bhtclau@cityu.edu.hk
†Electronic supplementary information (ESI) available. CCDC 2406139–2406142. For ESI and crystallographic data in CIF or other electronic format see DOI: https://doi.org/10.1039/d4qi03144j
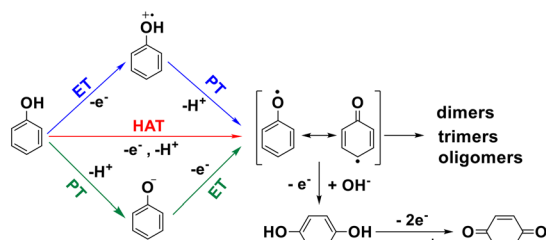
This journal is © the Partner Organisations 2025

Inorg. Chem. Front., 2025, **12**, 3157–3165 | 3157
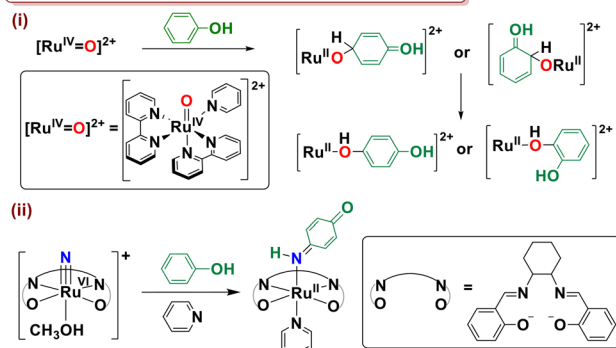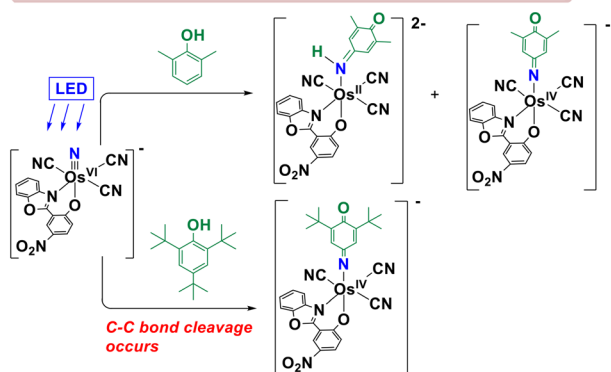
Fig. 1 Oxidation pathways of phenols by oxidants.

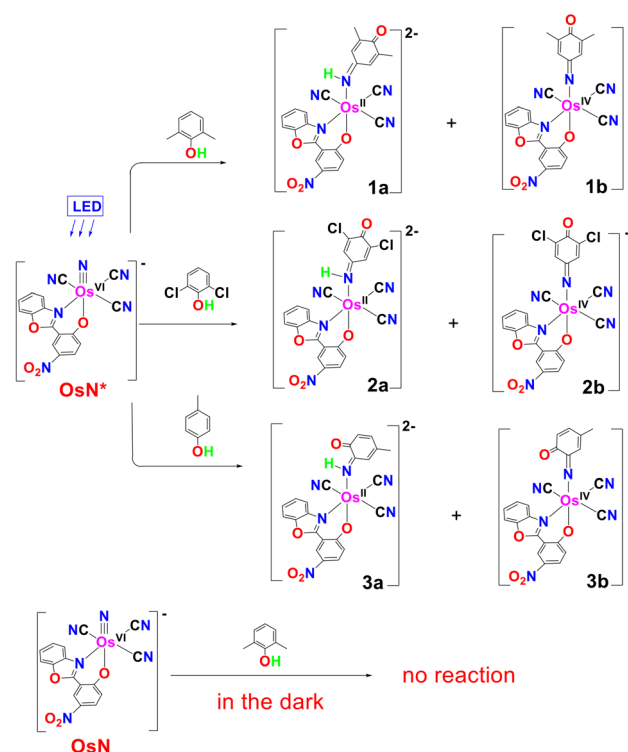(**OsN**, HL = 2-(2-hydroxy-5-nitrophenyl)benzoxazole);[26–33] **OsN** is highly luminescent in both solid state and fluid solution (solid state: λ_{em} = 591 nm, ϕ = 11.7%, τ = 1.90 µs; in degassed CH$_2$Cl$_2$: λ_{em} = 594 nm, ϕ = 3.0%, τ = 0.48 µs). The CV of **OsN** shows an irreversible oxidation wave at E_{pa} = 1.88 V and an irreversible reduction wave at E_{pa} = −0.99 V vs. Saturated Calomel Electrode (SCE), which are tentatively assigned as the metal-centered Os$^{VII/VI}$ and Os$^{VI/V}$ process, respectively. The excited state (**OsN***) of this complex is readily generated by visible light irradiation (λ > 460 nm). **OsN*** was found to be highly oxidizing and it reacts readily with various organic substrates, including alkanes, arenes, amines, alcohols, and dihydroxybenzenes.[26–33]

Herein, we reported the oxidation of phenols by **OsN***. These reactions have a number of unusual/novel features. In contrast to the oxidation of phenols by **RuN**, which occurs via

an electrophilic ring attack mechanism, oxidation by **OsN*** occurs by an ET-PT followed by an N-rebound mechanism. Similar to oxidation by **RuN**, oxidation of various mono- and di-substituted phenols by **OsN*** produced the corresponding osmium(II) benzoquinone imine complexes. However, because **OsN*** is a powerful oxidant, further oxidation of the osmium(II) products by **OsN*** occur to afford novel osmium(IV) iminato complexes as a second product. Moreover, oxidation of tri-substituted phenol such as 2,4,6-^{t}Bu$_3$C$_6$H$_2$OH results in C–C bond cleavage of the substrate.

Results and discussion

Upon irradiation with blue LED (λ > 460 nm) for 24 h, the light-yellow CH$_2$Cl$_2$ solution of **OsN** and 10 equiv. of 2,4,6-Me$_3$C$_6$H$_2$OH rapidly turned dark red (Fig. 2). A mixture of the osmium(II) p-benzoquinone monoimine complex [Os^{II}(L)(CN)$_3$(NH=Me$_2$Ph$_{(-2H)}$=O)]$^{2-}$ (**1a**) and osmium(IV) p-benzoquinone monoiminato complex [Os^{IV}(L)(CN)$_3$(N=Me$_2$Ph$_{(-2H)}$=O)]$^-$ (**1b**), were isolated as PPh$_4^+$ salts with 20% and 26% yields, respectively. Similarly, the photoreaction of **OsN** with 2,6-Cl$_2$C$_6$H$_3$OH afforded a mixture of (PPh$_4$)$_2$[Os^{II}(L)(CN)$_3$(NH=Cl$_2$Ph$_{(-2H)}$=O)] [(PPh$_4$)$_2$**2a**] and (PPh$_4$)[Os^{IV}(L)(CN)$_3$(N=Cl$_2$Ph$_{(-2H)}$=O)] [(PPh$_4$)**2b**] with 32% and 25% yields, respectively. In addition, (PPh$_4$)[Os^{II}(L)(CN)$_3$(NH$_3$)] (**OsNH$_3$**)[28] was isolated with ~10% yield in reactions with these phenols. Controlled experiments showed that

Fig. 2 Reactions of **OsN** with various phenols in the excited state and ground state.

3158 | Inorg. Chem. Front., 2025, **12**, 3157–3165

This journal is © the Partner Organisations 2025

no reaction between **OsN** and phenols was observed in the dark.

On the other hand, in the photoreaction with 4-methyl-phenol, **OsN** undergoes electrophilic attack at the *ortho* position to afford an $[PPh_4]_2[Os^{II}(L)(CN)_3(o\text{-}NH\!=\!MePh_{(-2H)}\!=\!O)]$ $[(PPh_4)_23a]$ and $[PPh_4][Os^{IV}(L)(CN)_3(o\text{-}N\!=\!MePh_{(-2H)}\!=\!O)]$ $[(PPh_4)3b]$, with yields of 37% and 32%, respectively.

The photoreactions of **OsN** with 2,4,6-tri-*tert*-butylphenol and 2,4,6-tri-methylphenol were also investigated (Fig. 3); for these substrates with three alkyl substituents, direct electrophilic attack on the aromatic ring by **OsN*** may be inhibited. Reaction of **OsN*** with $2,4,6\text{-}^tBu_3C_6H_2OH$ afforded $[Os^{IV}(L)(CN)_3(p\text{-}N\!=\!^tBu_2Ph_{(-2H)}\!=\!O)]^-$ (**4a**), isolated as PPh_4^+ salt with ~52% yield. The structure of **4a** (see characterization below) reveals formal C–C bond cleavage of $2,4,6\text{-}^tBu_3C_6H_2OH$; GC/MS and GC show that the 2-methylpropene was formed with ~50% yield. ^1H NMR spectrum of $(PPh_4)4a$ shows that the remaining two ^tBu groups are symmetry-related, consistent with the *para* attack of $2,4,6\text{-}^tBu_3C_6H_2OH$ by **OsN***. ESI/MS (−ve mode) of the photoreaction solution of **OsN** and $2,4,6\text{-}^tBu_3C_6H_2OH$ shows a predominant peak at m/z 743 (Fig. 4), attributed to $[Os^{IV}(L)(CN)_3(p\text{-}N\!=\!^tBu_2Ph_{(-2H)}\!=\!O)]^-$ (**4a**). There is also a very minor peak at m/z 801, (estimated to be 5%), which is tentatively assigned to $[Os^{IV}(L)(CN)_3(NH\text{-}^tBu_3Ph_{(-2H)}\!=\!O)]^-$ (**4b**), arising from an electrophilic attack of **OsN** at the *para* position of the phenol.

In the case of $2,4,6\text{-}Me_3C_6H_2OH$ with less bulky methyl substituents, electrophilic ring attack by **OsN*** occurred predominantly at the *para* position, and the amido complex, $[Os^{IV}(L)(CN)_3\{NH\text{-}(Me_3Ph_{(-2H)}\!=\!O)\}]^-$ (**5**), was isolated as PPh_4^+ salt with ~75% yield. The ESI/MS (−ve mode) of the product solution shows a predominant peak at m/z = 675 due to complex **5**. In addition, there are two minor peaks at m/z 659.1 and 275.6, which are tentatively assigned to **1b** and $[Os^{II}(L)(CN)_4]^{3-}$, respectively. These two species should arise from C–C bond cleavage of $2,4,6\text{-}Me_3C_6H_2OH$; however, the total yields of these two products are estimated to be <5%.
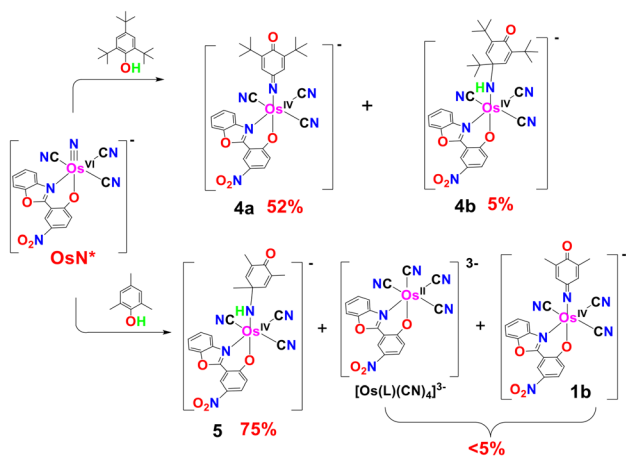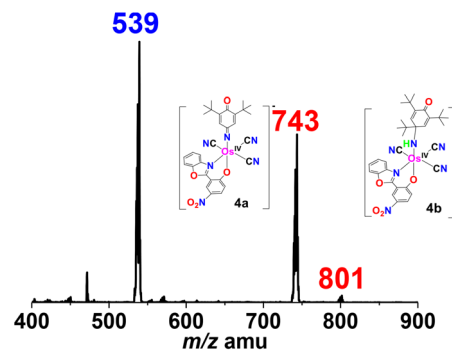

Fig. 4 ESI/MS of photoreaction of **OsN** with 10 equiv. $2,4,6\text{-}^tBu_3C_6H_2OH$ for 4 h showing a predominant peak at m/z 743 and a small peak at m/z 801.

All products have been characterized by IR, UV/vis, CV, ESI/MS, and ^1H NMR (Fig. S1–S12†). All the Os(II) and Os(IV) compounds are diamagnetic, as evidenced by the sharp resonances found in the normal range in their ^1H NMR spectra. The diamagnetism of these compounds is consistent with the low spin d^6 and d^4 electronic configurations for Os(II) and Os(IV), respectively. The IR spectra of $(PPh_4)_21a$ and $(PPh_4)_22a$ show $\nu(C\!\equiv\!N)$ stretches at 2096, 2070 cm^{-1} and 2108, 2082 cm^{-1}, and $\nu(C\!=\!O)$ stretches at 1609 cm^{-1} and 1610 cm^{-1}, respectively. The IR spectra of $(PPh_4)1b$ and $(PPh_4)2b$ show $\nu(C\!\equiv\!N)$ stretches at 2145, 2134 cm^{-1} and 2153, 2142 cm^{-1}, and $\nu(C\!=\!O)$ stretches at 1629 cm^{-1} and 1639 cm^{-1}, respectively which are at higher wavenumbers as compared with $(PPh_4)_21a$ and $(PPh_4)_22a$. Similar $\nu(C\!\equiv\!N)$ and $\nu(C\!=\!O)$ stretches are also found in $(PPh_4)_23a$ and $(PPh_4)3b$.

As shown in Fig. S6,† the UV/vis spectra of these compounds show ligand-centered $\pi-\pi^*$ transitions in the UV regions. In the osmium(II) products $(PPh_4)_21a$, $(PPh_4)_22a$, and $(PPh_4)_23a$, there are strong absorption bands at 500–650 nm with molar extinction coefficients (ε) of the order of 10^4 M^{-1} cm^{-1}, which are assigned to Os(II) to *p*-benzoquinone monoimine charge transfer (MLCT) transitions. Notably, there is an intense absorption band with $\varepsilon > 6 \times 10^4$ M^{-1} cm^{-1} in $(PPh_4)_22a$. In the osmium(IV) products $(PPh_4)1b$, $(PPh_4)2b$ and $(PPh_4)3b$, the broad absorption bands at ~450 nm are probably due to LMCT transitions.

The cyclic voltammograms (CVs) of the osmium complexes $(PPh_4)1a$, $(PPh_4)_22a$, and $(PPh_4)_23a$ in CH_3CN exhibit a reversible/quasi-reversible $Os^{III/II}$ couples at −0.67 V, −0.38 V and −0.78 V *vs.* $Fc^{+/0}$, respectively (Fig. 5). There is also an irreversible wave at E_{pc} = −1.46 V, −1.35 V and −1.72 V, respectively which are tentatively assigned to the reduction of the benzoquinone imine ligands. The oxidation waves at $E_{1/2}$ = 1.25 V, E_{pc} = 1.46 V and 1.23 V, respectively, are assigned to $Os^{IV/III}$. The CVs of the osmium(IV) products **1b**, **2b** and **3b** exhibit irreversible $Os^{IV/III}$ waves at E_p = −0.65 V, −0.39 V and −0.66 V, respectively (Fig. 6); while the waves at E_p = −1.61 V, −1.35 V and −1.49 V, respectively are tentatively assigned to the reduction of benzoquinone imine ligands.
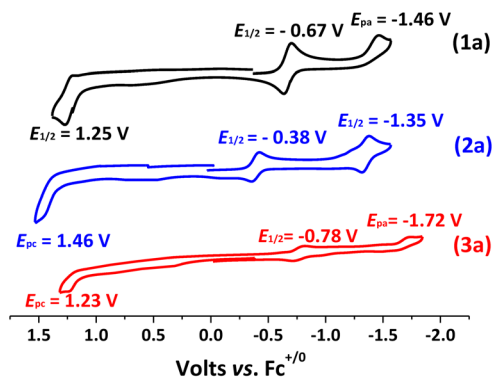

Fig. 3 Photoreaction of **OsN** with $2,4,6\text{-}^tBu_3C_6H_2OH$ and $2,4,6\text{-}Me_3C_6H_2OH$.

This journal is © the Partner Organisations 2025

Inorg. Chem. Front., 2025, **12**, 3157–3165 | **3159**

Fig. 5 CVs for **1a**, **2a**, and **3a** in MeCN solutions containing 0.1 M [^{n}Bu$_4$N](PF$_6$) with a scan rate = 0.1 V s^{-1}.

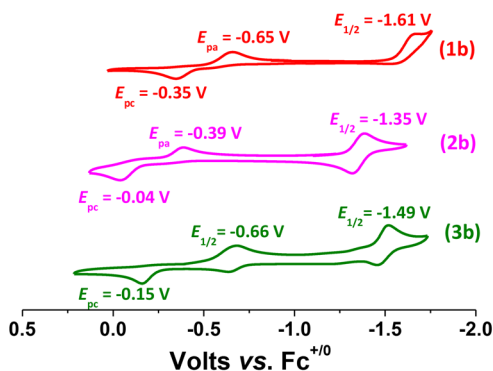**Fig. 6** CVs for **1b**, **2b**, and **3b** in MeCN solutions containing 0.1 M [^{n}Bu$_4$N](PF$_6$) with a scan rate = 0.1 V s^{-1}.
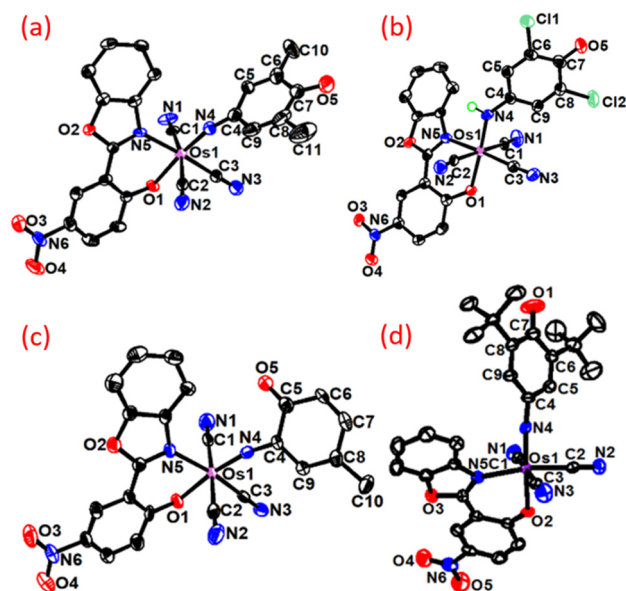

Fig. 7 The structures of (a) **1b**, (b) **2a**, (c) **3b** and (d) **4a**.

Table 1 Selected bond parameters (Å, °) for **1b**, **2a**, **3b** and **4a**

	1b	**2a**	**3b**	**4a**
Os1–C1	2.074 (5)	2.053 (4)	2.082 (5)	2.081(5)
Os1–C2	2.077 (5)	2.070 (4)	2.081 (5)	2.029(4)
Os1–C3	2.025 (5)	2.009 (4)	2.034 (6)	2.066(5)
Os1–N4	1.781 (4)	1.927 (3)	1.768 (4)	1.779(4)
Os1–N5	2.117 (4)	2.129 (3)	2.118 (4)	2.115(3)
Os1–O1	2.010 (3)	2.066 (3)	2.028 (3)	—
Os1–O2	—	—	—	2.022(3)
Os1–N4–C4	167.2 (4)	136.6 (3)	167.9 (5)	163.8(3)

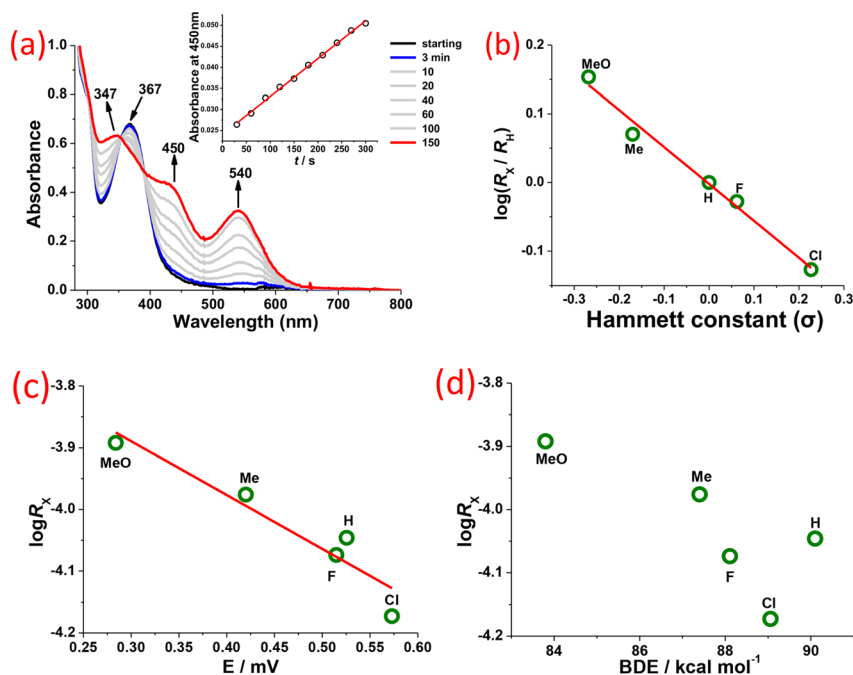**Fig. 8** (a) UV/vis spectral changes for the photoreaction of **OsN** (2.5 × 10^{-5} M) with phenol (1.8 × 10^{-3} M) in C$_2$H$_4$Cl$_2$. Inset shows the time-trace absorbance at 450 nm. (b) Hammett plot for the photoreaction of **OsN** with 4-substituted phenols in C$_2$H$_4$Cl$_2$. Slope = −0.54. Intercept = −0.00217. (c) Plot of log(R_x) vs. E^{ox}. (d) Plot of log(R_x) vs. BDE.

The molecular structures of **(PPh$_4$)1b**, **(PPh$_4$)$_2$2a**, **(PPh$_4$)3b**, and **(PPh$_4$)4a** have been determined by X-ray crystallography (Fig. 7). Selected bond parameters are summarized in Table 1. The *mer*-configuration of **OsN** is retained in these complexes. There are two PPh$_4^+$ in **2a** and only one PPh$_4^+$ in **1b** and **3b**. The Os–N4 bond length in **2a** is 1.927(3) Å, which is significantly shorter than related Os–N bond lengths in [Os^{III}\{N(H)C(NH$_2$)\}(L^1)(CN)$_3$]$^-$ and [Os^{III}\{N(H)CN\}(L^1)(CN)$_3$]$^{2-}$ (HL^1 = 2-(2-hydroxyphenyl)benzoxazole),[32,33] indicating the presence of strong π back-bonding interaction between Os^{II} and the benzoquinone monoimine ligand. On the other hand, the Os–N4 bond lengths are 1.781(4) and 1.768(4) Å, respectively for **1b** and **3b**, which are much shorter than that in **2a**, indicating Os–N double bond character in these Os(IV) complexes. This is also evidenced by the more linear Os1–N4–C4 bond angles of 167.2(4)° and 167.9(5)° than that in **2a** (136.6(3)°). The bond parameters of **3b** and **4a** are essentially identical to those in **1b**, as the metal centers have the same oxidation state.

Substituent effects

The photoreactions of **OsN** with various 4-substituted phenols (4-X-C$_6$H$_4$OH; X = MeO, Me, H, F, Cl) were also investigated by UV/vis spectroscopy (Fig. S10†). The initial rates (R_x) of these reactions were obtained at 450 nm (Fig. 8a). R_x was found to increase with increasing electron donating properties of the substituents: MeO > Me > H > F > Cl. A linear correlation was obtained in the Hammett plot of $\log(R_x/R_H)$ *versus* the substituent constant (σ), with a ρ value of -0.54 ± 0.01 (Fig. 8b), indicating that the phenol center is more positive in the transition state. $\log(R_x)$ also correlates well with the oxidation potentials (E^{ox}) of these phenols with a slope of -0.80 (Fig. 8c).[34] The results indicate that the reaction may proceed *via* an initial rate-limiting 1e$^-$ transfer (ET) from phenols to **OsN***. No clear correlation between $\log(R_x)$ and pK_a of phenols, suggesting that proton transfer (PT) is not involved in the rate-limiting step. There is also no clear relationship between $\log(R_x)$ and the O–H bond dissociation energies (BDEs) of the phenols (Fig. 8d),[35] which does not support a hydrogen atom transfer (HAT) mechanism for the oxidation of phenols by **OsN***.

Kinetic isotope effects (KIE)

The KIE for the reaction of **OsN*** with phenol was determined by ESI/MS, using an equimolar mixture of phenol (C$_6$H$_5$OH) and d^6-phenol (C$_6$D$_5$OD) as substrate. As shown in Fig. 9a, the KIE value was estimated to be ~(1 ± 0.05) from the ratios of the most intense peaks for two Os(IV) benzoquinone monoiminato products, (m/z = 631 and 635 for [Os^{IV}(L)(CN)$_3$(N=C$_6$H$_4$=O)]$^-$ and [Os^{IV}(L)(CN)$_3$(N=C$_6$D$_4$=O)]$^-$ respectively), assuming that the spraying and ionization efficiencies of the two ions are similar. The isotopic distribution pattern obtained is also in agreement with the simulated one. The KIE is also determined by UV/vis spectroscopy. As shown in Fig. S11,† the UV/vis spectral changes were obtained from the photoreaction of **OsN** with phenol (C$_6$H$_5$OH) and d^6-phenol (C$_6$D$_5$OD) under the same conditions. The reactions were followed by the change in absorbance at 367 nm, which gives a KIE of $R_H/R_D = 0.97 \pm$
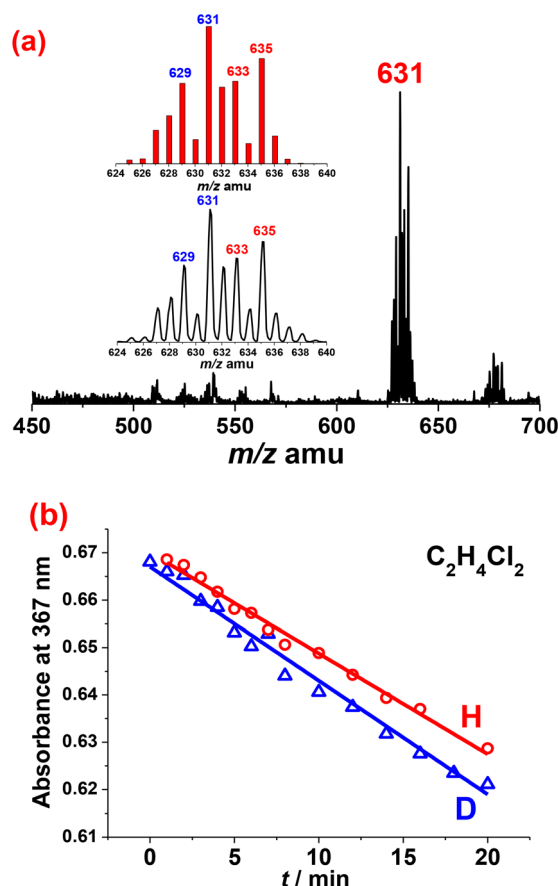

Fig. 9 (a) ESI/MS for the photoreaction of **OsN** with equimolar of phenol and d^6-phenol showing a predominant peak around m/z 631. Inserts show the expanded isotopic distribution of peak m/z 631, which agrees with the simulated isotopic distribution of m/z 631 and 635 with a mole ratio of 0.505 : 0.495 (KIE ~1). (b) Time trace for absorbance at 367 nm of **OsN** (2.5×10^{-5} M) with 100 equiv. of phenol (red line) and d^6-phenol (blue line) in C$_2$H$_4$Cl$_2$. The linear fitting gives initial rates of R_H = $(-2.13 \pm 0.06) \times 10^{-3}$, r^2 = 0.98 and R_D = $(-2.40 \pm 0.10) \times 10^{-3}$, r^2 = 0.99; $R_H : R_D$ = 0.97.

0.01 (Fig. 9b). Based on the above results, the photoreaction of **OsN** with phenol exhibits negligible KIE, indicating that C–H bond cleavage is not involved in the rate-limiting step, in line with the conclusion obtained from investigation of substituent effects.

Proposed mechanism

Based on the above experiments, the proposed mechanism for the photoreaction of **OsN** with phenols is illustrated in Fig. 10 (using 2,6-Me$_2$C$_6$H$_3$OH as an example). The initial step is rate-limiting 1e$^-$ oxidation of 2,6-Me$_2$C$_6$H$_3$OH (ET), followed by rapid proton transfer (PT) to give the **Os^{V}NH** and phenoxy radical, which is supported by a linear correlation between $\log(R_x)$ and E of the phenols with a slope of -0.80. The proposed mechanism is also supported by the linear Hammett correlation with ρ value of -0.54 and a negligible KIE effect (k(C$_6$H$_5$OH)/k(C$_6$D$_5$OD) ~1.03). Moreover, the initial rate (R) for phenolate is 60 times faster than that of phenol, further vali-

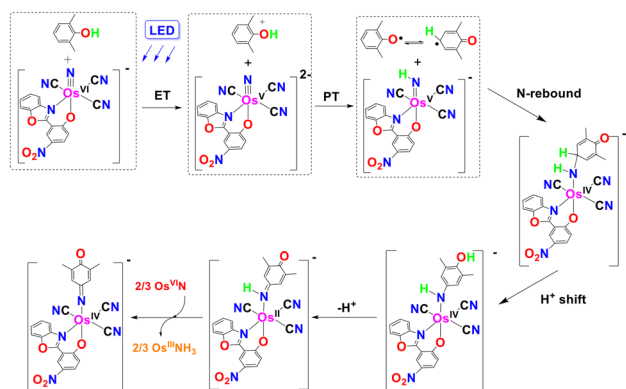This journal is © the Partner Organisations 2025

Inorg. Chem. Front., 2025, **12**, 3157–3165 | **3161**

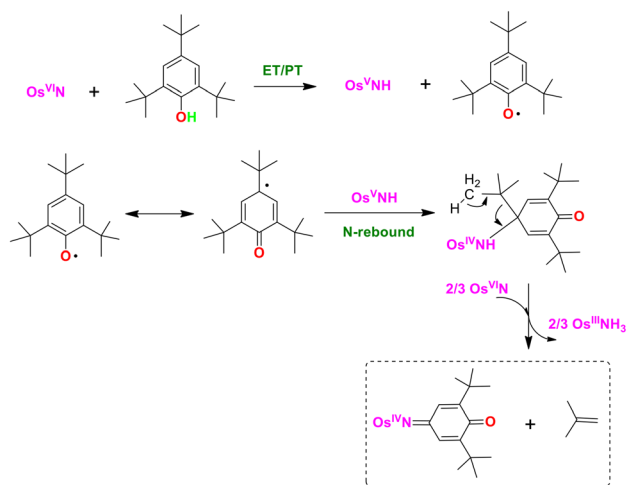**Fig. 10** The proposed reaction mechanism for the reaction of **OsN*** with 2,6-$Me_2C_6H_3OH$.

Fig. 11 The proposed mechanism for the C–C bond cleavage of 2,4,6-$^tBu_3C_6H_2OH$ by **OsN***.

dating the initial ET mechanism (Fig. S12†). This is followed by tautomerism and N-rebound to give an Os^{IV} amido species. An internal $2e^-$ redox results in the Os^{II} hydroquinone monoimine product. The other product, Os(IV) hydroquinone monoiminato complex, was formed by further $2e^-$ oxidation by **OsN*** ($2/3\mathbf{OsN^*} + \mathbf{1a} \rightarrow \mathbf{1b} + 2/3\mathbf{OsNH_3}$). This last step is supported by the isolation of **OsNH₃** in 10% yield.

For the photoreaction of **OsN** and 2,4,6-$^tBu_3C_6H_2OH$, the first four steps are similar (Fig. 11), *i.e.* $1e^-$ oxidation of 2,4,6-$^tBu_3C_6H_2OH$ (ET), followed by rapid proton transfer (PT) to give the **Os^VNH** and phenoxy radical; followed by tautomerism and N-rebound to give an Os^{IV} amido species. Further $2e^-$ oxidation of this Os^{IV} amido species by **OsN*** leads to C–C bond cleavage with the formation of **4a**, 2-methylpropene, and **OsNH₃**.

Conclusion

In conclusion, we have demonstrated novel reactivity of the excited state of an osmium(VI) nitrido complex towards phenols. The photoreactions of **OsN** with the parent phenol, as well as mono- and di-substituted phenols afforded Os(II) *p*-benzoquinone monoimine and osmium(IV) *p*-benzoquinone monoiminato complexes. On the other hand, oxidation of bulky tri-substituted phenol such as 2,4,6-$^tBu_3C_6H_2OH$ resulted in C–C bond cleavage of the substrate. Mechanistic studies indicate that the photoreactions proceed *via* an initial $1e^-$ oxidation followed by a rapid proton transfer (ET-PT) to generate phenoxy radicals, this is followed by a N-rebound step to give the osmium products. We believe that our work is a significant contribution to M≡N excited state as well as phenol oxidation chemistry.

Experimental

$(PPh_4)_2[Os^{II}(L)(CN)_3(NH=Me_2PhOH_{(-2H)})]$ [$(PPh_4)_2$1a] and $(PPh_4)[Os^{IV}(L)(CN)_3(N=Me_2PhOH_{(-2H)})]$ [(PPh_4)1b]

10 tubes each containing **OsN** (5 mg, 5.7 μmol) and 2,6-$Me_2C_6H_3OH$ (73 mg, 0.6 mmol) in CH_2Cl_2 under argon were irradiated with blue LED light for 24 h, whereby the light-yellow solutions turned dark red. The solutions were combined, and the solvent was removed under reduced pressure. The residue was washed with diethyl ether (100 ml) to remove the unreacted 2,6-$Me_2C_6H_3OH$. The residue was dissolved in a minimum amount of CH_2Cl_2 and then loaded onto a silica gel column. The first yellow band $(PPh_4)[Os^{IV}(L)(CN)_3(N=Me_2Ph_{(-2H)}=O)]$ [(PPh_4)1b] was eluted by CH_2Cl_2/acetone (v : v, 4 : 1). Yellow needle crystals were obtained from slow diffusion of diethyl ether into a MeCN solution of (PPh_4)1b. The second blue band was eluted by CH_2Cl_2/acetone/MeOH (v : v : v, 8 : 2 : 1). The solvent was removed under reduced pressure. The solid obtained was dissolved in H_2O (10 ml) and excess PPh_4Cl (30 mg) was added to give the blue precipitate. The crude product was further purified by slow diffusion of diethyl ether into a CH_2Cl_2 solution of $(PPh_4)_2$1a. Yield for $(PPh_4)_2$1a: 15 mg, 20% (based on the **OsN** consumed). Selected IR (KBr disc, cm^{-1}): ν(N–H) 3248; ν(C≡N) 2096 and 2070; ν(C=O) 1645; ν(C=N) 1609; ν(N=O) 1303. ^1H NMR (400 MHz, CDCl₃): δ 8.92 (s, 1H, Ar–H), 7.92–7.78 (m, 8H, Ar–H), 7.77–7.64 (m, 18H, Ar–H), 7.62–7.48 (m, 18H, Ar–H), 7.38 (d, J = 8.0 Hz, 1H, Ar–H), 7.29 (m, 1H, Ar–H), 7.19 (t, J = 8.0 Hz,1H, Ar–H), 6.67 (s, 1H, Ar–H), 1.69 (s, 6H). ESI/MS (−ve mode) in MeOH: at m/z 329.7 ([M]$^{2-}$); Anal. Calcd for $C_{72}H_{56}N_6O_5P_2Os$: C, 64.66; H, 4.22; N, 6.28. Found: C, 64.80; H, 4.25; N, 6.32%. UV/Vis (CH_2Cl_2): λ_{max} [nm] (ε [mol^{-1} dm^3 cm^{-1}]): 269 (22 472), 276 (21 630), 287 (16 020), 344 (14 050), 377sh (11 870), 432 (11 270), 541 (17 340), 586 (17 670). Yield for (PPh_4)1b: 15 mg, 26% (based on the **OsN** consumed). Selected IR (KBr disc, cm^{-1}): ν(C≡N) 2145 and 2135; ν(C=O) 1630; ν(C=N) 1611. ^1H NMR (400 MHz, CDCl₃): δ 9.04 (s, 1H, Ar–H), 8.19 (s, 2H, Ar–H), 8.07 (d, J = 9.5 Hz, 1H, Ar–H), 7.96–7.88 (m, 4H, Ar–H), 7.84–7.74 (m, 9H, Ar–H), 7.72 (d, J = 7.4 Hz, 1H, Ar–H), 7.69–7.61 (m, 8H, Ar–H), 7.53 (t, J = 8.3 Hz, 2H, Ar–H), 6.92 (d, J = 9.2 Hz, 1H, Ar–H), 3.15 (s, 6H, –CH₃). ESI-MS (−ve mode) in MeOH: m/z 659 (M⁻); Anal. Calcd for $C_{48}H_{35}N_6O_5OsP$: C, 57.82; H, 3.54; N, 8.43. Found: C, 57.93; H, 3.60; N, 8.31%. UV/Vis (CH_2Cl_2): λ_{max} [nm] (ε [mol^{-1}

3162 | *Inorg. Chem. Front.*, 2025, **12**, 3157–3165

This journal is © the Partner Organisations 2025

dm^3 cm^{-1}]): 269 (23 710), 277 (25 070), 288 (23 480), 330 (22 610), 432 (33 300).

(PPh$_4$)$_2$[Os^{II}(L)(CN)$_3$(NH=Cl$_2$PhOH$_{(-2H)}$)] [(PPh$_4$)$_2$2a] and (PPh$_4$)[Os^{IV}(L)(CN)$_3$(N=Cl$_2$PhOH$_{(-2H)}$)] [(PPh$_4$)2b]

The synthesis and isolation of (PPh$_4$)$_2$2a and (PPh$_4$)2b are similar to that of (PPh$_4$)$_2$1a and (PPh$_4$)1b except that 2,6-Cl$_2$C$_6$H$_3$OH was used instead of 2,6-dimethylphenol. Yield for (PPh$_4$)$_2$2a: (25 mg, 32%, based on the OsN consumed). Selected IR (KBr disc, cm^{-1}): ν(N–H) 3235; ν(C≡N) 2108 and 2082; ν(C=O) 1638; ν(C=N) 1609; ν(N=O) 1307; ^{1}H NMR (400 MHz, CDCl$_3$): δ 8.96 (d, J = 2.9 Hz, 1H), 7.90–7.82 (m, 8H), 7.80 (d, J = 2.9 Hz, 1H), 7.77–7.68 (m, 16 H), 7.65–7.56 (m, 16H), 7.55–7.48 (m, 2H), 7.37–7.29 (m, 3H), 7.23 (s, 1H); 6.78 (d, J = 9.4 Hz, 1H). ESI-MS (−ve mode) in MeOH: m/z 350.2 [M]$^{2-}$. Anal. Calcd for C$_{70}$H$_{50}$Cl$_2$N$_6$O$_5$OsP$_2$: C, 61.00; H, 3.66; N, 6.10. Found: C, 61.10; H, 3.71; N, 6.18%. UV/Vis (CH$_2$Cl$_2$): λ_{max} [nm] (ε [mol^{-1} dm^3 cm^{-1}]): 262sh (18 090), 269 (19 810), 276 (18 740), 285sh (12 760), 338 (12 110), 363sh (9360), 417sh (7070), 593 (60 850). Yield for (PPh$_4$)2b: 15 mg, 25% (based on the OsN consumed). Selected IR (KBr disc, cm^{-1}): ν(C≡N) 2153 and 2141; ν(C=O) 1639; ν(C=N) 1614. ^{1}H NMR (400 MHz, CDCl$_3$): δ 9.08 (s, 1H, Ar–H), 8.50 (s, 2H, Ar–H), 8.21 (d, J = 8.9 Hz, 1H, Ar–H), 7.97–7.89 (m, 4H, Ar–H), 7.84–7.75 (m, 9H, Ar–H), 7.72–7.58 (m, 11H, Ar–H), 7.13 (d, J = 9.2 Hz, 1H, Ar–H). ESI-MS (−ve mode) in MeOH: m/z 699 (M$^-$); Anal. Calcd for C$_{46}$H$_{29}$Cl$_2$N$_6$O$_5$OsP: C, 53.23; H, 2.82; N, 8.10. Found: C, 53.29; H, 2.76; N, 8.21%. UV/Vis (CH$_2$Cl$_2$): λ_{max} [nm] (ε [mol^{-1} dm^3 cm^{-1}]): 270 (40 050), 277 (44 140), 288sh (42 330), 331sh (37 880), 447 (60 490).

(PPh$_4$)$_2$[Os^{II}(L)(CN)$_3$(NH=MePhOH$_{(-2H)}$)] [(PPh$_4$)$_2$3a] and (PPh$_4$)[Os^{IV}(L)(CN)$_3$(N=MePhOH$_{(-2H)}$)] [(PPh$_4$)3b]

The synthesis and isolation of (PPh$_4$)$_2$3a and (PPh$_4$)3b are similar to that of (PPh$_4$)$_2$1a and (PPh$_4$)1b except that 4-MeC$_6$H$_4$OH was used instead of 2,6-Me$_2$C$_6$H$_3$OH. Yield for (PPh$_4$)$_2$3a, 28 mg, 37%. Selected IR (KBr disc, cm^{-1}) for (PPh$_4$)$_2$3a: ν(N–H) 3253; ν(C≡N) 2125 and 2086; ν(C=O) 1645; ν(C=N) 1612. ^{1}H NMR (400 MHz, CDCl$_3$): δ 9.03 (d, J = 2.9 Hz, 1H, Ar–H), 8.01 (s, 1H), 7.99 (s, 1H), 7.80–7.86 (m, 8H), 7.77–7.68 (m, 16 H), 7.65–7.56 (m, 16H), 7.18–7.10 (t, J = 8.0 Hz, 1H), 7.08 (d, J = 10.2 Hz, 1H), 6.72 (m, 2H), 6.38 (m, 2H), 5.32 (s, 1H) 1.27 (s, 3H), 3.50 (s, 3H, Me). ESI-MS (−ve mode) in MeOH: m/z 323.3 [M]$^{2-}$. Anal. Calcd for C$_{71}$H$_{54}$N$_6$O$_5$OsP$_2$: C, 64.44; H, 4.11; N, 6.35. Found: C, 64.10; H, 4.21; N, 6.18%. UV/Vis (CH$_2$Cl$_2$): λ_{max} [nm] (ε [mol^{-1} dm^3 cm^{-1}]): 262sh (18 090), 269 (19 810), 276 (18 740), 285sh (12 760), 338 (12 110), 363sh (9360), 417sh (7070), 593 (60 850). Yield for (PPh$_4$)3b, 18 mg, 32%. Selected IR (KBr disc, cm^{-1}): ν(C≡N) 2139 and 2130; ν(C=O) 1649; ν(C=N) 1614. ^{1}H NMR (400 MHz, CDCl$_3$): δ 9.07 (d, J = 2.8 Hz, 1H), 8.65 (dd, J = 6.3, 2.8 Hz, 1H) 8.13 (dd, J = 9.3, 2.9 Hz, 1H), 7.90–7.82 (m, 4H), 7.77–7.84 (m, 8H), 7.65–7.73 (m, 10H), 7.60–7.53 (m, 2H), 7.21 (dd, J = 9.8, 2.2 Hz, 1H), 6.99 (d, J = 9.3 Hz, 1H); 5.77 (d, J = 9.8 Hz, 1H) 3.58 (s, 3H). ESI-MS (−ve mode) in MeOH: m/z 645 [M]$^-$. Anal. Calcd for C$_{47}$H$_{33}$N$_6$O$_5$OsP: C, 57.43; H, 3.38; N, 8.55. Found: C, 57.10; H, 3.71; N, 8.18%. UV/Vis (CH$_2$Cl$_2$): λ_{max} [nm] (ε [mol^{-1} dm^3 cm^{-1}]): 262sh (18 090), 269 (19 810), 276 (18 740), 285sh (12 760), 338 (12 110), 363sh (9360), 417sh (7070), 593 (60 850).

(PPh$_4$)$_2$[Os^{IV}(L)(CN)$_3$(N=^{t}Bu$_2$Ph$_{(-2H)}$=O)] [(PPh$_4$)4a] and (PPh$_4$)[Os^{IV}(L)(CN)$_3$(NH-^{t}Bu$_3$PhOH$_{(-2H)}$)] [(PPh$_4$)4b]

The synthetic route of (PPh$_4$)4a and (PPh$_4$)4b is similar to that of (PPh$_4$)$_2$1a and (PPh$_4$)1b, except that the 2,4,6-^{t}Bu$_3$C$_6$H$_2$OH is used instead of 2,6-Me$_2$C$_6$H$_3$OH. The first yellow band (PPh$_4$)4a was eluted by CH$_2$Cl$_2$/acetone (v : v, 10 : 1). Yellow needle crystals were obtained from the slow diffusion of diethyl ether into an acetone solution of (PPh$_4$)4a. The solvent was removed under reduced pressure.

Yield for (PPh$_4$)4a: 32 mg, 52%. Selected IR (KBr disc, cm^{-1}): ν(C≡N) 2142 and 2128, ν(C=O) 1638; ν(C=N) 1615; ν(N=O) 1307. ^{1}H NMR (400 MHz, CDCl$_3$): δ 9.03 (d, J = 2.8 Hz, 1H, Ar–H), 8.12 (s, 2H, Ph–H), 8.05 (dd, J = 9.3, 2.9 Hz, 1H, Ar–H), 7.92 (dd, J = 8.0, 6.0 Hz, 4H, PPh$_4$-H), 7.83–7.76 (m, 9H, Ar–H and PPh$_4$-H), 7.73 (d, J = 7.2 Hz, 1H, Ar–H), 7.68–7.62 (m, 8H, PPh$_4$-H), 7.54 (dtd, J = 13.9, 7.8, 6.2 Hz, 2H, Ar–H), 6.89 (d, J = 9.4 Hz, 1H, Ar–H), 1.28 (s, 18H, CH$_3$). ESI-MS (−ve mode) in MeOH: m/z 743 [M]$^{2-}$. Anal. Calcd for C$_{54}$H$_{47}$N$_6$O$_5$OsP: C, 59.99; H, 4.38; N, 7.77. Found: C, 60.10; H, 4.31; N, 7.78%. UV/Vis (CH$_2$Cl$_2$): λ_{max} [nm] (ε [mol^{-1} dm^3 cm^{-1}]): 230 (27 380), 277 (15 620), 288 (14 640), 330 (13 030), 428 (20 930).

(PPh$_4$)[Os^{IV}(L)(CN)$_3$(NH-Me$_3$PhOH$_{(-H)}$)] [(PPh$_4$)5]

The synthetic route of (PPh$_4$)5 is similar to that of (PPh$_4$)$_2$1a and (PPh$_4$)1b, except that the 2,4,6-Me$_3$C$_6$H$_2$OH is used instead of 2,6-Me$_2$C$_6$H$_3$OH. (PPh$_4$)5 was purified by silica gel CH$_2$Cl$_2$/acetone (5 : 3) as the eluent. Yield: 43 mg, 75% (based on the OsN consumed). UV/Vis (CH$_2$Cl$_2$) for (PPh$_4$)5: λ_{max} [nm] (ε/M^{-1} cm^{-1}): 233 (42 430), 270 (18 030), 277 (19 430), 293 (20 360), 353 (20 460), 457 (6420). Selected IR (KBr disc, cm^{-1}) for 5: ν(C≡N) 2135 and 2127; ν(N–H) 3247; ν(C=N) 1610. ESI-MS (−ve mode) in MeOH: m/z 675 [M]$^-$. Anal. Calcd for C$_{49}$H$_{39}$N$_6$O$_5$OsP: C, 58.09; H, 3.88; N, 8.30. Found: C, 58.10; H, 3.81; N, 8.28%. ^{1}H NMR (400 MHz, CDCl$_3$): δ 8.93 (d, J = 2.8 Hz, 1H, Ar–H), 7.96 (d, J = 6.6 Hz, 1H, Ar–H), 7.89 (t, J = 7.2 Hz, 4H), 7.75 (td, J = 7.6, 3.7 Hz, 8H), 7.65–7.57 (m, 10H, Ar–H and PPh$_4$-H), 7.43 (t, J = 7.1 Hz, 1H, Ar–H), 7.20 (t, J = 8.4 Hz, 1H, Ar–H), 6.78 (s, 2H, Ph–H), 6.57 (d, J = 9.4 Hz, 1H, Ar–H), 2.23 (s, 3H, CH$_3$), 1.27 (s, 6H, CH$_3$).

Author contributions

The manuscript was written through contributions of all authors. All authors have given approval to the final version of the manuscript.

Data availability

The authors will supply the relevant data in response to reasonable requests.

This journal is © the Partner Organisations 2025

Inorg. Chem. Front., 2025, **12**, 3157–3165 | **3163**

Conflicts of interest

There are no conflicts to declare.

Acknowledgements

References

1 (a) J. Du Bois, C. S. Tomooka, J. Hong and E. M. Carreira, Nitridomanganese(v) Complexes: Design, Preparation, and Use as Nitrogen Atom-Transfer Reagents, *Acc. Chem. Res.*, 1997, **30**, 364–372; (b) J. T. Groves and T. Takahashi, Activation and transfer of nitrogen from a nitridomanganese(v) porphyrin complex. Aza analog of epoxidation, *J. Am. Chem. Soc.*, 1983, **105**, 2073–2074; (c) R. A. Eikey and M. M. Abu-Omar, Nitrido and imido transition metal complexes of Groups 6–8, *Coord. Chem. Rev.*, 2003, **243**, 83–124.

2 (a) J. F. Berry, Terminal Nitrido and Imido Complexes of the Late Transition Metals, *Comments Inorg. Chem.*, 2009, **30**, 28–66; (b) J. M. Smith, Reactive Transition Metal Nitride Complexes, *Prog. Inorg. Chem.*, 2014, **58**, 417–470; (c) M. N. Cosio and D. C. Powers, Prospects and challenges for nitrogen-atom transfer catalysis, *Nat. Rev. Chem.*, 2023, **7**, 424–438; (d) S. J. K. Forrest, B. Schluschaß, E. Y. Yuzik-Klimova and S. Schneider, Nitrogen Fixation via Splitting into Nitrido Complexes, *Chem. Rev.*, 2021, **121**, 6522–6587.

3 (a) T. J. Meyer and M. H. V. Huynh, The Remarkable Reactivity of High Oxidation State Ruthenium and Osmium Polypyridyl Complexes, *Inorg. Chem.*, 2003, **42**, 8140–8160; (b) T. J. Crevier and J. M. Mayer, Direct Attack of Phenyl Anion at an Electrophilic Osmium–Nitrido Ligand, *J. Am. Chem. Soc.*, 1998, **120**, 5595–5596; (c) S. N. Brown, Insertion of a Metal Nitride into Carbon–Carbon Double Bonds, *J. Am. Chem. Soc.*, 1999, **121**, 9752–9753.

4 (a) W.-L. Man, W. W. Y. Lam and T.-C. Lau, Reactivity of Nitrido Complexes of Ruthenium(vi), Osmium(vi), and Manganese(v) Bearing Schiff Base and Simple Anionic Ligands, *Acc. Chem. Res.*, 2014, **47**, 427–439; (b) W.-L. Man, W. W. Y. Lam, S.-M. Yiu, T.-C. Lau and S.-M. Peng, Direct Aziridination of Alkenes by a Cationic (Salen)ruthenium(vi) Nitrido Complex, *J. Am. Chem. Soc.*, 2004, **126**, 15336–15337; (c) W.-L. Man, W. W. Y. Lam, H.-K. Kwong, S.-M. Yiu and T.-C. Lau, Ligand-Accelerated Activation of Strong C-H Bonds of Alkanes by a (Salen)ruthenium(vi)–Nitrido Complex, *Angew. Chem., Int. Ed.*, 2012, **51**, 9101–9104.

5 (a) J. J. Scepaniak, C. S. Vogel, M. M. Khusniyarov, F. W. Heinemann, K. Meyer and J. M. Smith, Synthesis, Structure, and Reactivity of an Iron(v) Nitride, *Science*, 2011, **331**, 1049–1052; (b) S. B. Muñoz III, W.-T. Lee, D. A. Dickie, J. J. Scepaniak, D. Subedi, M. Pink, M. D. Johnson and J. M. Smith, Styrene Aziridination by Iron(iv) Nitrides, *Angew. Chem., Int. Ed.*, 2015, **54**, 10600–10603.

6 (a) H. Shi, H. K. Lee, Y. Pan, K.-C. Lau, S.-M. Yiu, W. W. Y. Lam, W.-L. Man and T.-C. Lau, Structure and reactivity of a manganese(vi) nitrido complex bearing a tetraamido macrocyclic ligand, *J. Am. Chem. Soc.*, 2021, **143**, 15863–15872; (b) H. Shi, R. Liang, D. L. Phillips, H. K. Lee, W.-L. Man, K.-C. Lau, S.-M. Yiu and T.-C. Lau, Structure and Reactivity of One- and Two-Electron Oxidized Manganese(v) Nitrido Complexes Bearing a Bulky Corrole Ligand, *J. Am. Chem. Soc.*, 2022, **144**, 7588–7593.

7 (a) G. W. Burton and K. U. Ingold, Vitamin E: application of the principles of physical organic chemistry to the exploration of its structure and function, *Acc. Chem. Res.*, 1986, **19**, 194; (b) L. Doyle, A. Magherusan, S. Xu, K. Murphy, E. R. Farquhar, F. Molton, C. Duboc, L. Que Jr. and A. R. McDonald, Class Ib Ribonucleotide Reductases: Activation of a Peroxido-Mn^{II}Mn^{III} to Generate a Reactive Oxo-Mn^{III}Mn^{IV} Oxidant, *Inorg. Chem.*, 2024, **63**, 2194–2203; (c) K. J. Fisher, M. L. Feuer, H. M. C. Lant, B. Q. Mercado, R. H. Crabtree and G. W. Brudvig, Concerted proton-electron transfer oxidation of phenols and hydrocarbons by a high-valent nickel complex, *Chem. Sci.*, 2020, **11**, 1683–1690.

8 C. Tommos and G. T. Babcock, Proton and hydrogen currents in photosynthetic water oxidation, *Biochim. Biophys. Acta, Bioenerg.*, 2000, **1458**, 199.

9 (a) S. Kundu, E. Miceli and E. R. Farquhar, Mechanism of phenol oxidation by heterodinuclear Ni Cu bis (μ-oxo) complexes involving nucleophilic oxo groups, *Dalton Trans.*, 2014, **43**, 4264–4267; (b) D. Dhar, G. M. Yee, T. F. Markle, J. M. Mayer and W. B. Tolman, Reactivity of the copper(iii)-hydroxide unit with phenols, *Chem. Sci.*, 2017, **8**, 1075–1085; (c) L. Yang, R. Ito, H. Sugimoto, Y. Morimoto and S. Itoh, Oxidation mechanism of phenols by copper(ii)–halide complexes, *Chem. Commun.*, 2024, **60**, 7586–7589; (d) J. Y. Lee, R. L. Peterson, K. Ohkubo, I. Garcia-Bosch, R. A. Himes, J. Woertink, C. D. Moore, E. I. Solomon, S. Fukuzumi and K. D. Karlin, Mechanistic Insights into the Oxidation of Substituted Phenols via Hydrogen Atom Abstraction by a Cupric–Superoxo Complex, *J. Am. Chem. Soc.*, 2014, **136**, 9925–9937.

10 (a) T. J. Meyer, M. H. V. Huynh and H. H. Thorp, The possible role of proton–coupled electron transfer (PCET) in water oxidation by photosystem II, *Angew. Chem., Int. Ed.*, 2007, **46**, 5284; (b) P. Mondal and A. R. McDonald, Phenol Oxidation by a Nickel(iii)–Fluoride Complex: Exploring the Influence of the Proton Accepting Ligand in PCET Oxidation, *Chem. – Eur. J.*, 2020, **26**, 10083–10089.

11 J. A. Stubbe, D. G. Nocera, C. S. Yee and M. C. Y. Chang, Radical initiation in the class I ribonucleotide reductase: long-range proton-coupled electron transfer?, *Chem. Rev.*, 2003, **103**, 2167.

3164 | *Inorg. Chem. Front.*, 2025, **12**, 3157–3165

This journal is © the Partner Organisations 2025

12 R. D. Webster, New insights into the oxidative electro-chemistry of vitamin E, *Acc. Chem. Res.*, 2007, **40**, 251.

13 M. H. V. Huynh and T. J. Meyer, Proton-coupled electron transfer, *Chem. Rev.*, 2007, **107**, 5004.

14 T. F. Markle, I. J. Rhile, A. G. DiPasquale and J. M. Mayer, Probing concerted proton–electron transfer in phenol–imidazoles, *Proc. Natl. Acad. Sci. U. S. A.*, 2008, **105**, 8185.

15 N. Song and D. M. Stanbury, Oxidation of Phenol by Tris (1, 10-phenanthroline) osmium(III), *Inorg. Chem.*, 2012, **51**, 4909.

16 J. Bonin, C. Costentin, C. Louault, M. Robert, M. Routier and J.-M. Savéant, Intrinsic reactivity and driving force dependence in concerted proton–electron transfers to water illustrated by phenol oxidation, *Proc. Natl. Acad. Sci. U. S. A.*, 2010, **107**, 3367.

17 A. Al-Ajlouni, A. Bakac and J. H. Espenson, Kinetics and mechanism of the oxidation of phenols by the oxochro-mium(IV) ion, *Inorg. Chem.*, 1993, **32**, 5792.

18 D. T. Y. Yiu, M. F. W. Lee, W. W. Y. Lam and T. C. Lau, Kinetics and mechanisms of the oxidation of phenols by a trans-dioxoruthenium(VI) complex, *Inorg. Chem.*, 2003, **42**, 1225.

19 T. Osako, K. Ohkubo and M. Taki, Oxidation mechanism of phenols by dicopper–dioxygen (Cu_2/O_2) complexes, *J. Am. Chem. Soc.*, 2003, **125**, 11027–11033.

20 D. E. Lansky and D. P. Goldberg, Hydrogen Atom Abstraction by a High-Valent Manganese(v)–Oxo Corrolazine, *Inorg. Chem.*, 2006, **45**, 5119–5125.

21 M. L. Neidig, A. Decker, O. W. Choroba, F. Huang, M. Kavana and G. R. Moran, Spectroscopic and electronic structure studies of aromatic electrophilic attack and hydrogen-atom abstraction by non-heme iron enzymes, *Proc. Natl. Acad. Sci. U. S. A.*, 2006, **103**, 12966–12973.

22 A. Gunay and K. H. Theopold, C–H Bond Activations by Metal Oxo Compounds, *Chem. Rev.*, 2010, **110**, 1060–1081.

23 W. K. Seok and T. J. Meyer, Multiple electron oxidation of phenols by an oxo complex of ruthenium(IV), *J. Am. Chem. Soc.*, 1988, **110**, 7358.

24 W. K. Seok, J. C. Dobson and T. J. Meyer, Mechanisms of oxidation of phenol and cyclohexene by an oxo complex of ruthenium(IV), *Inorg. Chem.*, 1988, **27**, 3–5.

25 J. H. Xie, W. L. Man, C. Y. Wong, X. Y. Chang, C. M. Che and T. C. Lau, Four-electron oxidation of phenols to p-benzoquinone imines by a (salen) ruthenium(VI) nitrido complex, *J. Am. Chem. Soc.*, 2016, **138**, 5817–5820.

26 (a) J. Xiang, X. X. Jin, Q. Q. Su, S. C. Cheng, C. C. Ko, W. L. Man, M. Y. Xue, L. L. Wu, C. M. Che and T. C. Lau, Photochemical nitrogenation of alkanes and arenes by a strongly luminescent osmium(VI) nitrido complex, *Commun. Chem.*, 2019, **2**, 40; (b) J. Xiang, H.-T. Shi, W.-L. Man and T.-C. Lau, Design of Highly Electrophilic and Stable Metal Nitrido Complexes, *Acc. Chem. Res.*, 2024, **57**, 2700–2716.

27 L. J. Luo, Q.-Q. Su, S. C. Cheng, J. Xiang, W. L. Man, W. M. Shu, M. H. Zeng, S. M. Yiu, C. C. Ko and T. C. Lau, Tunable luminescent properties of tricyanoosmium nitrido complexes bearing a chelating O^N ligand, *Inorg. Chem.*, 2020, **59**, 4406–4413.

28 (a) J. Xiang, Y. Pan, L.-L. Liu, L.-X. Wang, H. Yang, S.-C. Cheng, S.-M. Yiu, C.-F. Leung, C.-C. Ko, K.-C. Lau and T.-C. Lau, Visible Light-Induced Oxidation of Alcohols by a Luminescent Osmium(VI) Nitrido Complex: Evidence for the Generation of $PhIO^+$ as a Highly Active Oxidant in the Presence of PhIO, *J. Am. Chem. Soc.*, 2023, **145**, 9129–9135; (b) J. Xiang, M. Peng, Y. Pan, L. J. Luo, S. C. Cheng, X. X. Jin, S. M. Yiu, W. L. Man, C. C. Ko, K. C. Lau and T. C. Lau, Visible light-induced oxidative N-dealkylation of alkylamines by a luminescent osmium(VI) nitrido complex, *Chem. Sci.*, 2021, **12**, 14494–14498; (c) J. Xiang, J. Zhu, M.-M. Zhou, L.-L. Liu, L.-X. Wang, M. Peng, B.-S. Hou, S.-M. Yiu, W.-P. To, C.-M. Che, K.-C. Lau and T.-C. Lau, Oxidative C–O bond cleavage of dihydroxybenzenes and conversion of coordinated cyanide to carbon monoxide using a luminescent Os(VI) cyanonitrido complex, *Chem. Commun.*, 2022, **58**, 7988–7991.

29 (a) Q. Q. Su, K. Fan, X. D. Huang, J. Xiang, S. C. Cheng, C. C. Ko, L. M. Zheng, M. Kurmood and T. C. Lau, Field-induced slow magnetic relaxation in low-spin S= 1/2 mono-nuclear osmium(V) complexes, *Dalton Trans.*, 2020, **49**, 4084–4092; (b) L. L. Liu, L. X. Wang, M. Peng, J. Xiang, H. Yang, S. M. Yiu and T. C. Lau, Ring nitrogenation of aromatic amines by the excited state of an osmium(VI) nitrido complex, *Inorg. Chem.*, 2023, **62**, 1447–1454.

30 J. Xiang, W. L. Man, S. M. Yiu, S. M. Peng and T. C. Lau, Reaction of an osmium(VI) nitrido complex with cyanide: formation and reactivity of an osmium(III) hydrogen cyana-mide complex, *Chem. – Eur. J.*, 2011, **17**, 13044–13051.

31 J. Xiang, Q. Wang, S. M. Yiu, W. L. Man, H. K. Kwong and T. C. Lau, Aerobic oxidation of an osmium(III) N-hydroxyguanidine complex to give nitric oxide, *Inorg. Chem.*, 2016, **55**, 5056–5061.

32 J. Xiang, Q. Wang, S. M. Yiu and T. C. Lau, Dual pathways in the oxidation of an osmium(III) guanidine complex. for-mation of osmium(VI) nitrido and osmium nitrosyl complex, *Inorg. Chem.*, 2017, **56**, 2022–2028.

33 J. Xiang, Q.-Q. Su, L.-J. Luo and T.-C. Lau, Synthesis and reactivity of an osmium(III) aminoguanidine complex, *Dalton Trans.*, 2019, **48**, 11404–11410.

34 C. Li and M. Z. Hoffman, One-electron redox potentials of phenols in aqueous solution, *J. Phys. Chem. B*, 1999, **103**, 6653–6656.

35 J. H. Xie, L. Ma, W. W. Y. Lam, K. C. Lau and T. C. Lau, Hydrogen atom transfer reactions of ferrate(VI) with phenols and hydroquinone. Correlation of rate constants with bond strengths and application of the Marcus cross relation, *Dalton Trans.*, 2016, **45**, 70–73.

This journal is © the Partner Organisations 2025

Inorg. Chem. Front., 2025, **12**, 3157–3165 | **3165**